MIDLINE BRAIN INJURY IN THE IMMATURE RAT INDUCES SUSTAINED COGNITIVE DEFICITS, BIHEMISPHERIC AXONAL INJURY AND NEURODEGENERATION

Jimmy W. Huh[1], **Ashley G. Widing**[2], and **Ramesh Raghupathi**[2],*

[1]*Department of Anesthesiology and Critical Care, Children's Hospital of Philadelphia, Philadelphia, PA 19104*

[2]*Department of Neurobiology and Anatomy, Drexel University College of Medicine, Philadelphia, PA 19129*

Abstract

Infants and children less than 4 years old suffer chronic cognitive deficits following mild, moderate or severe diffuse traumatic brain injury (TBI). It has been suggested that the underlying neuropathologic basis for behavioral deficits following severe TBI is acute brain swelling, subarachnoid hemorrhage and axonal injury. To better understand mechanisms of cognitive dysfunction in mild-moderate TBI, a closed head injury model of midline TBI in the immature rat was developed. Following an impact over the midline suture of the intact skull, 17-day-old rats exhibited short apnea times (3–15 seconds), did not require ventilatory support and suffered no mortality, suggestive of mild TBI. Compared to un-injured rats, brain-injured rats exhibited significant learning deficits over the first week post-injury (P<0.0005), and, significant learning (P<0.005) and memory deficits (P<0.05) in the third post-injury week. Between 6 and 72h, blood-brain barrier breakdown, extensive traumatic axonal injury in the subcortical white matter and thalamus, and focal areas of neurodegeneration in the cortex and hippocampus were observed in <u>both</u> hemispheres of the injured brain. At 8 to 18 days post-injury, reactive astrocytosis in the cortex, axonal degeneration in the subcortical white matter tracts, and degeneration of neuronal cell bodies and processes in the thalamus of <u>both</u> hemispheres were observed; however, cortical volumes were not different between un-injured and injured rat brains. These data suggest that diffuse TBI in the immature rat can lead to ongoing degeneration of both cell soma and axonal compartments of neurons, which may contribute, in part, to the observed sustained cognitive deficits.

Traumatic brain injury (TBI) remains a leading cause of acquired brain damage and death in children; in particular, children less than 4 years of age have higher rates of TBI-related hospitalization, morbidity, and mortality than older children (Langlois et al., 2003; Langlois et al., 2005; Levin et al., 1992). While severe TBI in children is almost always associated with

*Address correspondence to: Ramesh Raghupathi, Ph.D., Department of Neurobiology and Anatomy, Drexel University College of Medicine, 2900 Queen Lane, Philadelphia, PA 19129, T: 215-991-8405, F: 215-843-9082, E-mail: rramesh@drexelmed.edu.

chronic cognitive deficits (Ewing-Cobbs et al., 2006; Anderson et al., 2005), it is becoming increasingly evident that mild to moderate trauma in children (which occurs at a greater incidence rate than severe TBI) can also result in chronic cognitive dysfunction (Beers, 1992; Wrightson et al., 1995). Irrespective of injury severity, the most common pathologic entity that has been described following diffuse brain injury in children is traumatic axonal injury (TAI, Babikian et al., 2005; Ciurea et al., 2005; Tong et al., 2004; Chiaretti et al., 1998). To better understand mechanisms of cognitive deficits associated with mild to moderate diffuse brain injury, it is imperative to develop a clinically-relevant and injury-severity appropriate model of pediatric TBI.

Experimental models of mild to moderate pediatric diffuse TBI have been developed in the 17–19 day-old rat or in the 3–5 day-old pig (neurologically equivalent to a toddler), although there is substantial variance with respect to behavioral deficits and pathologic alterations. Mild to moderate lateral fluid-percussion brain trauma in the 17-or 19-day-old rat resulted in mild cognitive dysfunction in the acute but not in the chronic post-traumatic period in the absence of overt cell loss and TAI (Prins and Hovda, 1998; Gurkoff et al., 2006). However, lateral fluid-percussion brain trauma in the immature rat did result in transient calcium accumulation, hyperglycolysis and a few eosinophilic neurons in the cortex immediately below the impact site (Osteen et al., 2001; Thomas et al., 2000; Gurkoff et al., 2006). More recently, we have demonstrated that lateral concussive brain trauma in the 17-day-old rat did not affect learning of a spatially-oriented task but did lead to retention deficits at 4 weeks post-injury (Raghupathi and Huh, 2007). Mild TAI was observed in and restricted to the thalamus and subcortical white matter tracts below the impact site at 3 days post-injury, which was resolved by day 14 (Raghupathi and Huh, 2007). Non-impact, axial rotation of the head of the 3–5 day-old piglet at moderate severity, but not mild severity, induced TAI in multiple white matter tracts throughout the brain and led to behavioral deficits over the first 12 days post-injury (Raghupathi et al., 2004; Friess et al., 2007). Moderate weight-drop trauma over the midline suture of the immature rat resulted in minimal physiologic alterations; acute and long-term cognitive and motor function deficits and TAI (in midline structures) were only observed following ultra-severe diffuse brain trauma (Adelson et al., 1996; Adelson et al., 1997; Adelson et al., 2000; Adelson et al., 2001). These data underscore the importance of injury severity and histologic damage in both hemispheres of the brain (diffuse injury) as potential mechanisms for post-traumatic behavioral dysfunction.

Our objective was to develop a closed head injury model of mild-moderate severity that would result in histologic alterations in both hemispheres of the immature rodent brain and lead to acute and sustained cognitive deficits. To this end, the electronically-driven controlled cortical impact (CCI) device was used to deliver an impact over the midline suture of the intact skull in free-standing 17-day-old rats. We evaluated learning and memory functions using the Morris water maze in the 1st week and 3rd week post-traumatic period, and examined injured brains for evidence of neurodegeneration (using Fluoro-Jade B), blood-brain barrier breakdown (BBB), astrocytic reactivity and TAI (using immunohistochemistry for amyloid precursor protein, APP).

Methods

Brain Injury

The numbers of animals used in the present study are described in Table 1. Brain injuries were induced using the electronically driven controlled cortical impact (eCCI) device (Custom Design International, Richmond, VA), a modification of the pneumatic CCI previously described (Dixon et al., 1991) and used in previous studies in immature rats (Huh and Raghupathi, 2007;Raghupathi and Huh, 2007). The metal indentor was convex, measured 5mm in diameter and was driven with a velocity of 5m/sec with a dwell time of 100msec. Seventeen

day old male and female Sprague-Dawley (Charles River Laboratories, Wilmington, MA) rat pups (N=38, 33 ± 4g, mean ± standard deviation (SD)) were anesthetized with isofluorane (5%) using a nose cone, and, once a loss of a tail-pinch reflex was observed, a midline incision was made to expose the skull. The periosteum was reflected and the animal was placed in a standard mouse restrainer (Braintree Scientific, Braintree, MA); the head was supported by a soft foam pad in order to make it level with the body. The restrainer was positioned under the CCI device, the nose cone was removed, and the site of impact over the midline suture was marked on the intact skull using a felt-tipped pen, exactly at the center point between the lambda and bregma sutures. At about 45 seconds after removal of anesthesia (by which time the animals exhibited minimal pain reflex), rats were subjected to an impact, where the indenter traveled a distance of 3mm into the skull. Immediately following the impact, the animals were monitored for length of apnea, length of loss of righting reflex and the return of pain reflex. Sham-injured animals (N=33, 33 ± 5g) were anesthetized with isofluorane (5%) via a nose cone, their scalps were opened, they were placed in the restrainer, the nose cone was removed, and the impactor tip was zeroed on the skull. The total time from initiation of anesthesia to removal of the nose cone prior to the zeroing of the impactor tip to the surface of the skull was 4 minutes. Apnea latency times were recorded for injured animals from the time of impact to when they returned to normal, spontaneous breathing. The loss of a righting reflex was measured by the length of time taken by the animal to return onto all four limbs after being placed on their side immediately following injury. The return of the pain reflex was evaluated by the latency required by the animal to withdraw its hind limb following a toe pinch. Once the animal regained normal breathing, the skull was evaluated for the presence of fracture, herniation, and hematoma. Herniation was evident from the extrusion of brain tissue through the fracture, while a hematoma was defined on the basis of the presence and location of a discoloration under the skull by visual observations. Hematomas were classified as either, mild: little to no discoloration at or around the site of impact, moderate: presence of discoloration at the impact site, or severe: bilateral discoloration present in regions adjacent to impact site in addition to the injured area. Following recovery from injury/anesthesia, the animals were re-anesthetized with isofluorane in order to suture the scalp, and the pups were returned to the dam. Animals were placed on a heating pad maintained at 37°C to maintain body temperature throughout the procedures and recovery. Pups were weaned from the dam on postnatal day 21. All surgical and behavioral procedures were done in accordance with the rules and regulations of the Institutional Animal Care and Use Committee of Drexel University College of Medicine and were in compliance with the Guide for the Care and Use of Animals.

Cognitive function

Cognitive function was assessed in separate groups of injured and sham animals on days 4–8 or days 14–18 days post-injury (N=13 injured and 10 sham animals per testing time point), by an evaluator who was blinded to the injury status of the animals and the testing time point. In the acquisition task, the length of time taken (latency) for the animal to locate a submerged, hidden platform in the Morris water maze (MWM) was recorded (Morris et al., 1982). The water maze consisted of a 1-meter diameter circular pool containing water at 18°C and made opaque using non-toxic white paint, and an eccentrically-placed platform submerged 1 cm below the surface of the water. Rats were placed in the center of the pool and guided towards the fixed start points located on the periphery of the maze which were separated by 90°. The animals were required to locate the hidden platform using visual cues placed outside and around the pool. Each rat was subjected to 4 trials a day for 4 consecutive training days (days 4–7 or days 14–17). The animals that did not find the platform in the allotted time (60 seconds) were placed upon it for 15 seconds (for trial 1 of each day) or 5 seconds (for each subsequent trial) and those that did were allowed to remain on the platform for 5 seconds. Animals were allowed to dry between trials by placement under a heat lamp. The average latency to reach the platform

on each training day (average of 4 trials) was computed and the data is presented as a function of training day in order to determine the learning component of the task.

At 24 hours following the last training trial day (days 8 or 18), spatial memory (retention) was tested in the probe trials during which the platform was removed from the maze. Each rat underwent a total of 2 probe trials of 60 seconds each, with an inter-trial interval of approximately 15 minutes. All animals were placed in the pool in the same manner as they were during training, with starting points being the two furthest from the location of the platform. The swimming pattern was recorded using a CCD camera and the time spent in various zones (zone A being closest to the platform and zone G being the perimeter of the maze) surrounding the platform location was computed (AccuScan, San Diego Instruments, San Diego CA)(Saatman et al., 2006). Animals received a score calculated using the formula previously described (Smith et al., 1991):

[time spent in zone A * 20] + [time spent in zone B * 5] + [time spent in zone C *2] + [(time spent in zone D/time spent in zone G) * 35].

The final memory score represented the average of the scores received in the 2 probe trials. The swim speed of the animal during each probe trial was also assessed. After the probe trials, the platform was placed back in the maze at the same location, except that it was now 2 cm above the surface of the water (visible platform trial) and a visual cue was adhered to the platform. The latency of the animal to reach the platform was measured.

Tissue preparation for immunohistochemistry and histology

At 6h, 1, 3, 8 and 18 days, sham- and brain-injured animals (see Table 1 for N's) were anesthetized (sodium pentobarbital, 60mg/Kg, i.p.) and euthanized by trans-cardial perfusion with 4% paraformaldehyde. Brains were post-fixed in the skull for 24 hours, then post-fixed outside the cranial cavity for an additional 24 hours, cryoprotected in 30% sucrose, and frozen in liquid isopentane at −35°C. Coronal (40 µm thick) sections were taken every 0.5 mm between bregma and −4.3 mm posterior to bregma. Each "set" contained 10 sections. One set of sections were mounted on gelatin-coated slides and stained with 2% Cresyl violet and 0.2% Cyanin R (Nissl-Myelin) for assessment of gross histology. Additional sets of adjacent sections were evaluated for reactive astrocytosis (anti-glial fibrillary acidic protein, GFAP, clone GA5, Sigma Chemical Co., St. Louis, MO; 1:1000), evidence of breakdown of the blood-brain barrier (biotinylated donkey anti-rat IgG, Jackson ImmunoResearch, West Grove, PA; 1:20,000), and traumatic axonal injury (polyclonal antibody to C-terminus of APP, Zymed, San Francisco, CA; 1:2000). For anti-APP immunohistochemistry, antigen retrieval was effected by incubating sections in 10mM sodium citrate (pH 6.5) at 60°C for 20min. Primary antibody binding was detected using a biotinylated donkey anti-rabbit IgG for C-terminus APP (Jackson ImmunoResearch, West Grove, PA; 1:1000) or biotinylated donkey anti-mouse IgG for GFAP (Jackson ImmunoResearch, West Grove, PA; 1:5000). Endogenous peroxidases were quenched by incubating tissue sections in 3 % hydrogen peroxide in 10 % methanol and Tris-buffered saline. Primary and secondary antibody complexes were visualized using the ABC Elite system (Vector Laboratories, Burlingame, CA) with diaminobenzidine (Vector) as chromogen. As negative control, 1–2 sections from each animal were incubated with secondary antibody and the ABC reagent prior to exposure to DAB. Tissue sections that were evaluated for APP were also counterstained with hematoxylin (1:10 of Gill-1, Thermo Shandon, Pittsburgh, PA).

Degeneration of both neuronal cell bodies and axons was evaluated using histochemistry with Fluoro-Jade B as previously described (Tong et al., 2002). Briefly, sections were mounted on gelatin-coated slides and allowed to dry at 4°C for 3–4 days. Sections were dehydrated and hydrated with graded ethanols, rinsed with dH_2O and impregnated in 0.06% potassium

permanganate for 20 minutes on a rocker. After 20 minutes, the tissue was washed with dH$_2$O, immersed in 0.001% Fluoro-Jade B (Chemicon, Temecula, CA) with 0.1% acetic acid for 30 minutes and washed in dH$_2$O. Slides were dried in a convection oven set at 60°C for 30 minutes, the tissue was cleared in Shandon xylene substitute and coverslipped with DPX mounting medium (Electron Microscopy Sciences, Hatfield, PA). Sections were analyzed using an Eclipse E400 microscope (Nikon Corporation).

Quantification of cortical tissue loss

The extent of cortical tissue loss was quantified using Nissl-stained sections (N=4–5 brain-injured and 2 sham animals at 8 and 18 days post-injury) as previously described (Huh and Raghupathi, 2007; Raghupathi and Huh, 2007). Sections were captured at 1X magnification using an Eclipse E400 microscope (Nikon Corporation) and digitized as TIFF images using Nikon ACT-1 software version 2.62 (Nikon). The area of the cortex, beginning at the midline and extending until the rhinal fissure with the grey-white matter interface serving as the inner boundary, was measured using NIH Image J (Rasband, 2007). The area measurements reflected that of the tissue that was stained with cresyl Violet and did not take the intensity of staining into account. Cortical tissue volume was calculated for each hemisphere and compared to the corresponding hemisphere in sham animals using the following formula:

$$\sum (\{[(A_i + A_{i+1})]/2\} * d_{i \to i+1})$$

where A_i = area of the cortex in section "i", A_{i+1} = area of the injured cortex in the next section from "i", $d_{i \to i+1}$ is the distance between sections "i" and the next section "i+1".

Statistical Analysis

All mean values are expressed as mean ± standard deviation (SD). Latencies to locate the hidden platform in the Morris water maze were compared using repeated measures analysis of variance (ANOVA, Injury Status X Training Days). Times of apnea, return of pain and righting reflexes, and cortical volumes were compared using a multiple ANOVA (MANOVA) as a function of time of euthanasia. Probe scores, latency to the visible platform, and swim speed were compared using the Student's t-test between sham and injured animals for each of the two time points evaluated. Post-hoc comparisons between groups were performed using the Newman-Keul's test. Differences were considered significant at $P < 0.05$. In all analyses, gender was used as a covariate.

Results

Midline impact results in skull fractures and brief apnea

Closed head injury with the metal-tipped indenter over the midline suture in the PND17 rat did not result in acute or delayed mortality. Impact resulted in linear skull fractures along the suture line in all injured animals (Table 2). In 5 injured animals (1 each at 6 hour and 8 day survival times and 3 at the 18 day survival time), a slight herniation of the brain through the midline fracture was observed. In all remaining injured animals, severe discoloration was observed under the site of impact (indicative of hematoma) (Table 2). Injury resulted in a brief period of apnea (3–15 seconds) that was not different between the groups euthanized at various times. However, the return of pain and righting reflexes were not different between sham- and brain-injured animals, suggesting that the recovery from anesthesia overwhelmed any effect of the brain injury (data not shown).

Midline impact results in acute and sustained acquisition deficits

In the acute post-traumatic period (days 4–7), midline impact in the PND17 rat resulted in acquisition deficits in the Morris water maze (Figure 1A). Although both sham- and brain-injured rats were able to locate the hidden platform over the 4-day learning period, repeated measures ANOVA revealed an INJURY (F (1,21) = 28.18, P<0.0001) and a DAYS (F (3,63) = 29.02, P<0.0001) effect, but not an interaction effect (INJURY × DAYS, F (3,63) = 0.49, P=0.69), suggesting that the rate of learning was not affected by the injury status of the animal. Post-hoc analyses for INJURY demonstrated a significant learning deficit in the brain-injured group (P<0.0005) across all training days. Midline impact in the 17-day-old animal resulted in sustained learning (acquisition) deficits, as evaluated in a separate group of sham and brain-injured rats in the third week post-injury. As illustrated in Figure 1B, both sham- and brain-injured animals were able to learn the location of the hidden platform over the 4-day learning period, beginning on day 14 post-injury/surgery. As observed in the acutely tested group, a repeated measures ANOVA revealed an INJURY effect (F (1,21) = 12.50, P<0.002) and a DAYS effect (F (3,63) = 28.38, P<0.00001) but not an interaction effect (INJURY × DAYS, F (3,63) = 1.06, P=0.37). Post-hoc analyses for INJURY revealed a significant deficit in the brain-injured group compared to the sham group across all training days (P<0.005). At both times of testing, the swim speed of brain-injured rats across all training days were not significantly different from those of the sham rats, suggesting that motor function deficits, if present, were not an underlying reason for the longer times taken by the brain-injured rats to reach the hidden platform (data not shown).

Despite the presence of an acquisition deficit at the acute time period post-injury, there was no significant difference in the probe trial scores between sham and brain-injured animals on day 8 post-injury (Table 3, F (1,21) = 1.53, P=0.24). In contrast, the acquisition deficit observed at the later time point was associated with a significant retention deficit on day 18 post-injury (F (1,21) = 5.35, P<0.05). The times taken by all rats to reach the visible platform were not significantly different from each other, suggesting that there were no visual impairments in the brain-injured rats. In addition, swim speeds were not significantly different between sham and brain-injured animals, indicative of the fact that motor function deficits, if present, were not an underlying cause for the observed retention deficits.

Midline impact results in traumatic axonal injury in both hemispheres

Subcortical white matter tracts—Intra-axonal accumulation of APP, indicative of impaired axonal transport (one phenotype of TAI), was observed in multiple white matter tracts in both hemispheres of the immature rat brain (Figure 2). While sham-injured animals did not reveal any APP staining in axons (Figures 2A–C), traumatic axonal injury was observed as early as 6 hours post-injury and appeared predominantly as APP(+) swellings within the cingulum (Figure 2D and J), lateral subcortical white matter tracts (Figure 2E and K) and corpus callosum (Figure 2F). At higher magnification, APP (+) swellings can be visualized in contiguous axons (arrowheads in panels J and K) or in terminal bulbs (arrows in panels J and L). Moreover, multiple APP(+) swellings were observed within a single axon as illustrated in Figure 2J (boxed area).

At 3 days post-injury, terminal bulbs were still visible in the subcortical white matter tracts, albeit to a more limited extent compared to the earlier post-injury times (Figures 3A–C). At 8 days post-injury, few, if any APP(+) injured axons were visible (data not shown); however, at this time, a number of Fluoro-Jade B-labeled axonal profiles were visible (Figures 3D–F), indicative of axonal degeneration as suggested by Tong et al (2002). By 18 days, the extent of Fluoro-Jade staining in the subcortical white matter tracts was decreased (data not shown). Sham-injured animals did not reveal any Fluoro-Jade staining in the subcortical white matter tracts (Figures 3G–I).

Thalamus—Compared to sham animals (Figure 4A), accumulation of APP in injured axons was sporadically observed at 6 hours post-injury in the thalamus of both right (Figure 4B) and left hemispheres (data not shown). By 24 hours (not shown) and 3 days post-injury (Figure 4C), TAI was not observed in any thalamic nucleus. Fluoro-Jade B labeling was not present in the sham animal (Figure 4D). However, extensive staining with Fluoro-Jade B was observed at 3 (Figure 4E) and 8 days post-injury (Figure 4F) in the thalamus of both hemispheres. At 3 days, Fluoro Jade labeling appeared mostly in axonal profiles (Figure 4E), while at 8 days, a few neurons, and degenerating axons and dendrites were Fluoro Jade B-positive (Figure 4F). By 18 days, Fluoro-Jade reactivity, although present, was substantially less (data not shown).

Midline impact results in blood-brain barrier breakdown, neurodegeneration and reactive astrocytosis

Cortex—Microscopic evaluation of Nissl-Myelin stained sections revealed that midline impact resulted in subpial and intraparenchymal hemorrhage (Figure 5A), which may arise due to tearing of the sinus and/or meningeal arteries; hemorrhage was not evident at 3 days post-injury (Figure 5B). Cortical and white matter tissue tears were observed below the site of impact in both hemispheres at 6 hours post-injury (Figure 5A), but by 18 days post-injury, both hemispheres looked morphologically normal without any evidence of contusion or demyelination of the white matter tracts (Figure 5C). Based on volumetric measurements of the cortex in the left and right hemispheres in sham- and brain-injured animals at 8 and 18 days post-injury, midline impact in the 17-day-old rat did not result in loss of tissue. In the left hemisphere, the cortical volume for sham animals (111.3 ± 2.4mm^3, mean $\pm$ SD), was not significantly different from those in brain-injured animals at either 8 days (108.0 ± 11.8 mm^3) or 18 days post-injury (105.7 ± 2.2mm^3). Similarly, in the right hemisphere, the cortical volumes for sham (110.7 ± 2.6mm^3), and brain-injured rats at 8 (107.4 ± 9.7mm^3) and 18 day post-injury (104.5 ± 7.2mm^3) were comparable to each other.

The presence of IgG immunoreactivity within gray matter and white matter tracts, indicative of blood-brain barrier breakdown, was observed as early as 6 hours directly below the impact site (Figure 5D), was maximal at 24 hours (Figure 5E), and substantially decreased by 3 days (Figure 5F) post-injury. Immediately adjacent to the areas within the cortex where hemorrhage, tissue tears and BBB breakdown was observed, Fluoro-Jade B-labeled neurons were visible in both hemispheres between 6 to 24 hours post-injury (Figures 5G, 5H). These labeled neurons were minimally present at 3 days post-injury (Figure 5I). Subsequent to neurodegeneration and BBB breakdown at 6 and 24 hours post-injury, reactive astrogliosis (as evidenced by GFAP immunoreactivity) was observed at 3 (Figure 5K) and 8 days post-injury (Figure 5L). The extent of GFAP immunoreactivity in the cortex at 24 hours (Figure 5J) was comparable to that observed in sham-injured animals (inset in Figure 5L).

Hippocampus—Midline impact on the intact skull of the 17-day-old rat resulted in neurodegeneration within the dentate gyrus in both hemispheres (Figure 6). Fluoro-Jade B-labeled neurons were observed in the hilus of the dentate gyrus and in the granule cell layer at 6 (data not shown) and 24 hours post-injury (Figure 6B). By 3 days post-injury, few, if any, degenerating neurons were observed (data not shown). However, by 8 days, fluoro-Jade B reactivity was observed in cells within the hilus that exhibited non-neuronal morphology (Figure 6C). In sham-injured animals, fluoro-Jade B staining was detected to a mild extent in cells with astrocytic morphology, as previously reported following focal ischemia (Butler et al., 2002) (Figure 6A). However, the extent of reactive astrogliosis in the hilus of the dentate gyrus was qualitatively similar between sham animals (Figures 6D) and brain-injured animals at 24 hours (Figure 6E) and 8 days post-injury (Figure 6F). No evidence of fluoro-Jade B reactivity was observed in the pyramidal cell layer of the hippocampus.

Summary of pathophysiologic alterations

Figure 7 illustrates the regional distribution and temporal progression of pathologic changes observed in the 17-day-old rat brain following an impact over the midline suture. At 6 – 24 hours (panels A-C), the injury is characterized by IgG extravasation in the grey and white matter tracts below the site of impact, APP accumulation in intact axons and terminal bulbs within the cingulum, corpus callosum, lateral white matter tracts and thalamus, and, neurodegeneration in the cortex, hilus of the dentate gyrus and thalamus. By 3 – 8 days, the only pathologic entities that are visible are increased reactive astrocytosis in the cortex below the impact site and Fluoro-Jade B-labeled axonal profiles within white matter tracts and the thalamus (panels D-F). These pathologic alterations are associated with learning but not retention deficits (Figure 1A and Table 3). By 18 days post-injury, a few degenerating axons, labeled with Fluoro- Jade B, remain within white matter tracts and the thalamus (panels G-I), and were associated with learning and memory deficits (Figure 1B and Table 3).

Discussion

The present study demonstrates that impact over the midline suture of the intact skull of the 17-day-old rat resulted in cognitive deficits within the first week post-injury, which was sustained until the third week post-injury. These behavioral deficits were accompanied, in the acute post-traumatic period (6 hours – 3 days) by blood-brain barrier breakdown, neurodegeneration in the cortex and hippocampus, and traumatic axonal injury (TAI) in the subcortical white matter and thalamus in <u>both</u> hemispheres of the injured brain. In the subacute post-traumatic period (8 – 18 days), degeneration of neuronal cell bodies and processes in the thalamus and axonal degeneration in the subcortical white matter tracts, and, increased reactive astrocytosis in the cortex of both hemispheres were observed. In the present study, all brain-injured animals sustained skull fractures following the impact, typically along the midline suture. Despite this, we did not observe an overt contusion in the cortex or hemispheric tissue loss. Moreover, the extent of apnea was comparable to previously published reports of mild TBI in the immature rat (Gurkoff et al., 2006). The absence of any mortality, losses of pain and righting reflexes, and that none of the brain-injured rats required ventilatory support, suggest that midline impact of 3mm distance into the intact skull generally results in mild, diffuse TBI in the 17-day-old rat; in a small subset of brain-injured animals (5 of 38), herniation of the brain was observed.

Sustained Learning and Memory Deficits

Testing in the Morris water maze on days 4–7 post-injury revealed significant acquisition deficits in brain-injured rats compared to their un-injured counterparts; however, these acquisition deficits did not translate into retention deficits, as both sham-and brain-injured rats were able to recall the location of the hidden platform with equal efficiency in the probe trial. These data are similar to those reported by Gurkoff and colleagues, where rats subjected to lateral fluid-percussion brain trauma on PND 19 exhibited learning deficits on days 6 and 7 post-injury, but no retention deficits at 2 weeks post-injury (Gurkoff et al., 2006). Our current data also revealed acquisition deficits during testing on days 14–17 post-injury, and retention (memory) deficits 24 hours later. Previous studies with unilateral non-contusive brain injury in PND 17 rats exhibited retention, but not acquisition deficits at chronic post-injury times (Prins and Hovda, 1998; Raghupathi and Huh, 2007). Both acquisition and retention deficits have been reported following ultra-severe weight drop injury in PND 17 rats, in which the animals had to be tracheally intubated and mechanically ventilated prior to injury (Adelson et al., 2000). To the best of our knowledge, the current data are the first to demonstrate that mild TBI results in learning deficits in the PND17 rat in both acute and subacute survival times. Moreover, the observation of retention deficits only at the later survival time suggests that brain injury early in development may demonstrate more profound cognitive deficits with maturity,

an idea that is consistent with observations that brain injury in infants and toddlers interferes with acquisition of new cognitive skills and results in more profound chronic neurobehavioral impairments (Taylor and Alden, 1997). Over time, the poor acquisition skills and memory impairment results in increased intellectual discrepancies between the head-injured child and age-matched normal peers (Anderson et al. 2000).

Bihemispheric traumatic axonal injury and neurodegeneration

Traumatic axonal injury (TAI), the pathologic hallmark of diffuse pediatric TBI, was observed predominantly in multiple subcortical white matter tracts of <u>both</u> hemispheres in our current study, and minimally in the thalamus and brainstem. Consistent with this, multiple clinical reports have shown that infants and children with TAI in the subcortical white matter tracts often have poor outcome (Ciurea et al., 2005; Grados et al., 2001; Tong et al., 2004). In contrast, midline weight drop injury did result in considerable axonal damage predominantly in the brainstem, and to a minimal extent in the corpus callosum (Adelson et al., 2001), indicative of the differences in mechanism of the primary injury; nevertheless, both models result in sustained learning and memory deficits. While the anatomical basis for post-traumatic cognitive deficits has yet to be defined, it is plausible that TAI leading to axonal degeneration in both hemispheres may contribute to cognitive dysfunction following diffuse brain injury in the immature animals. In part, these observations may explain the absence of sustained cognitive deficits following lateral, non-contusive brain injury, where axonal injury was observed only in the subcortical white matter tracts within injured hemisphere (Raghupathi and Huh, 2007). The absence of overt evidence of demyelination may be indicative of the small population of traumatically-injured axons, but does underscore the importance of utilizing electron microscopy to accurately and extensively assess axonal degeneration. While TAI was sporadically observed in the thalamus of both hemispheres during the acute (6 hours – 3 days) post-traumatic period, a more profound and delayed degeneration of neuronal cell bodies and processes were evident in the thalamus in the subacute (8 – 18 days) post-traumatic period. These observations of delayed neurodegeneration in the thalamus are consistent with those in other rodent models of pediatric traumatic and hypoxic-ischemic brain injury (Tong et al., 2002; Northington et al., 2001) and may be due to retrograde axonal degeneration of thalamo-cortical connections (Iizuka et al., 1990; Pierce et al., 1998). It is tempting to speculate that this progressive, ongoing, and diffuse neuronal and axonal degeneration may contribute to the greater cognitive deficits that were observed during the subacute post-traumatic period.

The observations of subpial and intracortical hemorrhages, tissue tears and blood-brain barrier breakdown in the acute post-injury period may be related to the presence of Fluoro-Jade B-labeled, degenerating neurons in the cortex. Despite the acute presence of degenerating neurons, there was little to no gross alterations in the tissue at 18 days post-injury, suggesting that the extent of neuronal loss was not sufficient to create a necrotic cavity. Similarly, acute degeneration of neurons was also observed in the granule cell layer and the hilus of the dentate gyrus in the hippocampus in both hemispheres; however, no overt loss of neurons was observed in the hippocampus at any survival time. Similarly, lateral fluid-percussion brain trauma in the immature rat did not induce significant loss of hippocampal neurons, measured using sensitive stereological techniques (Gurkoff et al., 2006). It is well known that the hippocampus plays an important role in spatial learning and memory (Morris et al., 1982). While these data underscore the vulnerable nature of the neurons within the dentate gyrus following TBI (Lowenstein et al., 1992), it is likely that neuronal dysfunction may, in part, contribute to cognitive deficits following diffuse brain trauma in the immature rat, which is consistent with previous published studies (Adelson et al., 2001; Fineman et al., 2000; Gurkoff et al., 2006; Prins et al., 1996; Raghupathi and Huh, 2007). Importantly, these observations underscore the importance of evaluating the presence of focal neuronal loss which may be a component of diffuse TBI in the immature rat.

While the mechanisms underlying acute neurodegeneration following experimental pediatric TBI are poorly understood, both excitotoxicity – leading to activation of proteases such as calpains and caspases - and inflammation – resulting in cytokine release and free radical generation - may play a role. Breakdown of the BBB and neurodegeneration may lead to the observed increases in astrocytic reactivity, which could further augment the toxic environment of the neurons. Furthermore, microglial activation may contribute to the on-going neuronal and axonal degeneration that is observed during the subacute post-traumatic period.

Conclusion

We have developed a clinically-relevant model of closed head injury in the immature rat that exhibits diffuse histopathologic alterations in both hemispheres of the injured brain, and, acute and sustained cognitive deficits. Furthermore, the ongoing pathogenesis following diffuse injury in the immature brain suggest an extended critical window of opportunity for therapy, once a better understanding of the underlying cellular mechanisms associated with progressive pathogenesis is elucidated.

Acknowledgement

Reference List

Adelson PD, Dixon CE, Kochanek PM. Long-term dysfunction following diffuse traumatic brain injury in the immature rat. J Neurotrauma 2000;17:273–282. [PubMed: 10776912]

Adelson PD, Dixon CE, Robichaud P, Kochanek PM. Motor and cognitive functional deficits following diffuse traumatic brain injury in the immature rat. J Neurotrauma 1997;14:99–108. [PubMed: 9069441]

Adelson PD, Jenkins LW, Hamilton RL, Robichaud P, Tran MP, Kochanek PM. Histopathologic response of the immature rat to diffuse traumatic brain injury. J Neurotrauma 2001;18:967–976. [PubMed: 11686497]

Adelson PD, Robichaud P, Hamilton RL, Kochanek PM. A model of diffuse traumatic brain injury in the immature rat. J Neurosurg 1996;85:877–884. [PubMed: 8893727]

Anderson V, Catroppa C, Morse S, Haritou F, Rosenfeld J. Functional plasticity or vulnerability after early brain injury? Pediatrics 2005;116:1374–1382. [PubMed: 16322161]

Anderson V, Catroppa C, Rosenfeld J, Haritou F, Morse SA. Recovery of memory function following traumatic brain injury in pre-school children. Brain Injury 2000;14:679–692. [PubMed: 10969886]

Babikian T, Freier MC, Tong KA, Nickerson JP, Wall CJ, Holshouser BA, Burley T, Riggs ML, Ashwal S. Susceptibility weighted imaging: neuropsychologic outcome and pediatric head injury. Pediatr.Neurol 2005;33:184–194. [PubMed: 16139733]

Beers SR. Cognitive effects of mild head injury in children and adolescents. Neuropsychol.Rev 1992;3:281–320. [PubMed: 1284851]

Butler TL, Kassed CA, Sanberg PR, Willing AE, Pennypacker KR. Neurodegeneration in the rat hippocampus and striatum after middle cerebral artery occlusion. Brain Res 2002;929:252–260. [PubMed: 11864631]

Chiaretti A, Visocchi M, Viola L, De BR, Langer A, Tortorolo L, Piastra M, Polidori G. Diffuse axonal lesions in childhood. Pediatr.Med Chir 1998;20:393–397. [PubMed: 10335538]

Ciurea AV, Coman T, Rosu L, Ciurea J, Baiasu S. Severe brain injuries in children. Acta Neurochir.Suppl 2005;93:209–212. [PubMed: 15986758]

Dixon CE, Clifton GL, Lighthall JW, Yaghmai AA, Hayes RL. A Controlled Cortical Impact Model of Traumatic Brain Injury in the Rat. J Neurosci Meth 1991;39:253–262.

Ewing-Cobbs L, Prasad MR, Kramer L, Cox CS Jr, Baumgartner J, Fletcher S, Mendez D, Barnes M, Zhang X, Swank P. Late intellectual and academic outcomes following traumatic brain injury sustained during early childhood. J Neurosurg 2006;105:287–296. [PubMed: 17328279]

Fineman I, Giza CC, Nahed BV, Lee SM, Hovda DA. Inhibition of neocortical plasticity during development by a moderate concussive brain injury. J Neurotrauma 2000;17:739–749. [PubMed: 11011814]

Friess SH, Ichord RN, Owens K, Ralston J, Rizol R, Overall KL, Smith C, Helfaer MA, Margulies SS. Neurobehavioral functional deficits following closed head injury in the neonatal pig. Exp Neurol 2007;204:234–243. [PubMed: 17174304]

Grados MA, Slomine BS, Gerring JP, Vasa R, Bryan N, Denckla MB. Depth of lesion model in children and adolescents with moderate to severe traumatic brain injury: use of SPGR MRI to predict severity and outcome. J Neurol Neurosurg Psychiatry 2001;70:350–358. [PubMed: 11181858]

Gurkoff GG, Giza CC, Hovda DA. Lateral fluid percussion injury in the developing rat causes an acute, mild behavioral dysfunction in the absence of significant cell death. Brain Res 2006;1077:24–36. [PubMed: 16490184]

Huh JW, Raghupathi R. Chronic cognitive deficits and long-term histopathological alterations following contusive brain injury in the immature rat. J Neurotrauma 2007;24:1460–1474. [PubMed: 17892408]

Iizuka H, Sakatani K, Young W. Neural damage in the rat thalamus after cortical infarcts. Stroke 1990;21:790–794. [PubMed: 1692645]

Langlois JA, Kegler SR, Butler JA, Gotsch KE, Johnson RL, Reichard AA, Webb KW, Coronado VG, Selassie AW, Thurman DJ. Traumatic brain injury-related hospital discharges. Results from a 14-state surveillance system, 1997. MMWR Surveill Summ 2003;52:1–20. [PubMed: 12836629]

Langlois JA, Rutland-Brown W, Thomas KE. The incidence of traumatic brain injury among children in the United States: differences by race. J Head Trauma Rehabil 2005;20:229–238. [PubMed: 15908823]

Levin HS, Aldrich EF, Saydjari C, Eisenberg HM, Foulkes MA, Bellefleur M, Luerssen TG, Jane JA, Marmarou A, Marshall LF. Severe head injury in children: experience of the Traumatic Coma Data Bank. Neurosurg 1992;31:435–443.

Lowenstein DH, Thomas MJ, Smith DH, McIntosh TK. Selective vulnerability of dentate hilar neurons following TBI : a potential mechanistic link between head trauma and disorders of the hippocampus. J Neurosci 1992;12:4846–4853. [PubMed: 1464770]

Morris RGM, Garrud P, Rawlins JNP, O'Keefe J. Place navigation impaired in rats with hippocampal lesions. Nature 1982;297:681–683. [PubMed: 7088155]

Northington FJ, Ferriero DM, Flock DL, Martin LJ. Delayed neurodegeneration in neonatal rat thalamus after hypoxia-ischemia is apoptosis. J Neurosci 2001;21:1931–1938. [PubMed: 11245678]

Osteen CL, Moore AH, Prins ML, Hovda DA. Age-dependency of 45calcium accumulation following lateral fluid percussion: acute and delayed patterns. J Neurotrauma 2001;18:141–162. [PubMed: 11229708]

Pierce JES, Smith DH, Trojanowski JQ, McIntosh TK. Enduring cognitive, neurobehavioral and histopathological changes persist for up to one year following experimental brain injury in rats. Neurosci 1998;87:359–369.

Prins ML, Hovda DA. Traumatic brain injury in the developing rat: effects of maturation on Morris water maze acquisition. J Neurotrauma 1998;15:799–811. [PubMed: 9814636]

Prins ML, Lee SM, Cheng CLY, Becker DP, Hovda DA. Fluid percussion brain injury in the developing and adult rat: a comparative study of mortality, morphology, intracranial pressure and mean arterial blood pressure. Dev Brain Res 1996;95:272–282. [PubMed: 8874903]

Raghupathi R, Huh JW. Diffuse brain injury in the immature rat: evidence for an age-at-injury effect on cognitive function and histopathologic damage. J Neurotrauma 2007;24:1596–1608. [PubMed: 17970623]

Raghupathi R, Mehr M, Helfaer MA, Margulies SS. Traumatic axonal injury is exacerbated following repetitive closed head injury in the neonatal pig. J Neurotrauma 2004;21:307–316. [PubMed: 15115605]

Rasband, WS.; Image, J. Bethesda, Maryland, USA: U. S. National Institutes of Health; 1997–2007. http://rsb.info.nih.gov/ij/,

Saatman KE, Feeko KJ, Pape RL, Raghupathi R. Differential behavioral and histopathological responses to graded cortical impact injury in mice. J Neurotrauma 2006;23:1241–1253. [PubMed: 16928182]

Smith DH, Okiyama K, Thomas MJ, Claussen B, McIntosh TK. Evaluation of Memory Dysfunction Following Experimental Brain Injury Using the Morris Water Maze. J Neurotrauma 1991;8(4):259–269. [PubMed: 1803034]

Taylor HG, Alden J. Age-related differences in outcomes following childhood brain insults: an introduction and overview. J Int.Neuropsychol.Soc 1997;3:555–567. [PubMed: 9448369]

Thomas S, Prins ML, Samii M, Hovda DA. Cerebral Metabolic Response to Traumatic Brain Injury Sustained Early in Development: A 2-Deoxy-D-Glucose Autoradiographic Study. J Neurotrauma 2000;17:649–665. [PubMed: 10972242]

Tong KA, Ashwal S, Holshouser BA, Nickerson JP, Wall CJ, Shutter LA, Osterdock RJ, Haacke EM, Kido D. Diffuse axonal injury in children: clinical correlation with hemorrhagic lesions. Ann Neurol 2004;56:36–50. [PubMed: 15236400]

Tong W, Igarashi T, Ferriero DM, Noble LJ. Traumatic brain injury in the immature mouse brain: characterization of regional vulnerability. Exp Neurol 2002;176:105–116. [PubMed: 12093087]

Wrightson P, McGinn V, Gronwall D. Mild head injury in preschool children: evidence that it can be associated with a persisting cognitive defect. J Neurol Neurosurg Psychiatry 1995;59:375–380. [PubMed: 7561915]
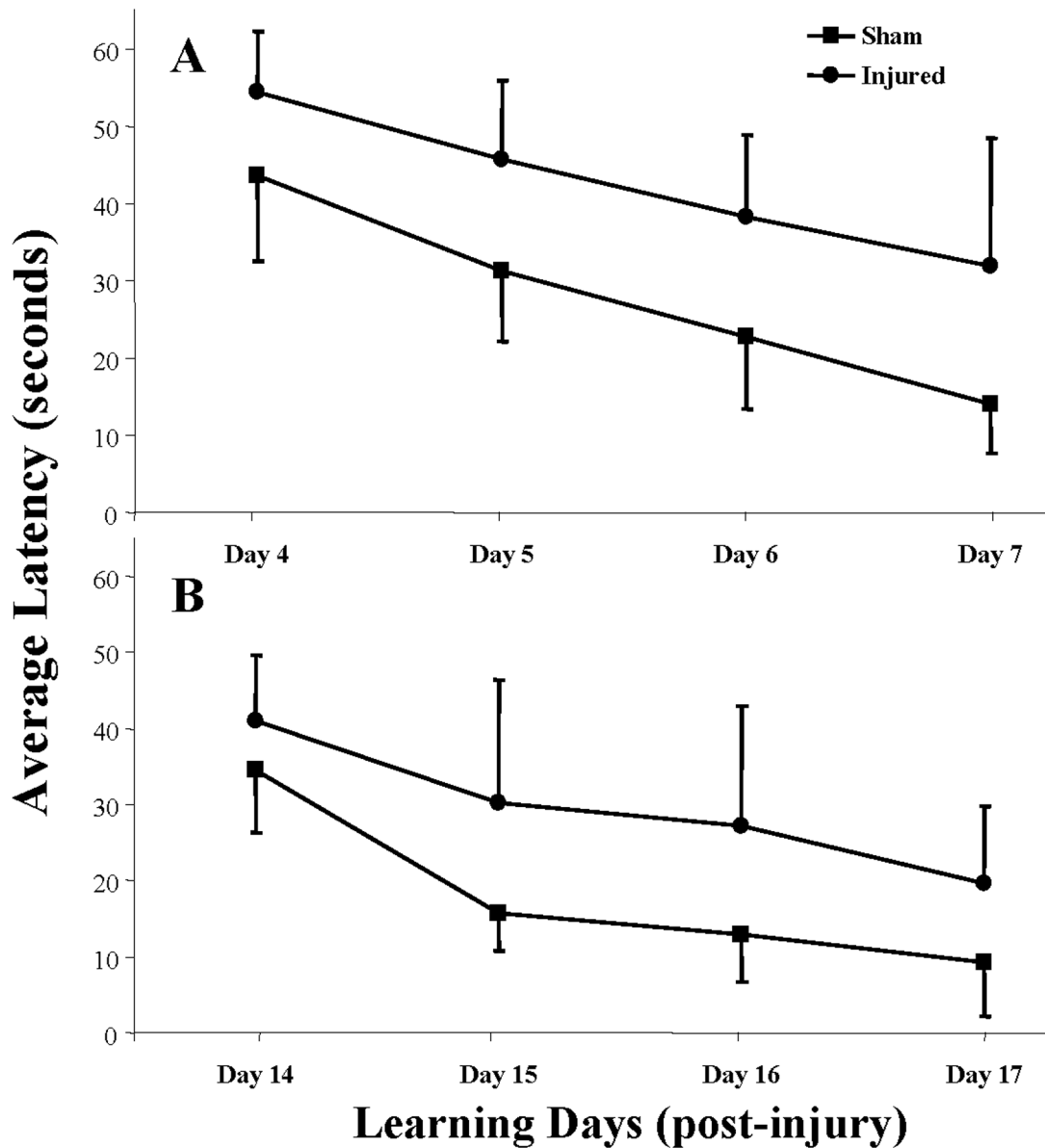
Figure 1. Acute and sustained learning deficits following midline brain injury in PND17 rats
Rats were tested in the Morris water maze for their ability to locate a hidden platform over the first week (panel A) and third week (panel B) post-injury as described in Methods. Data are presented as average latencies for each block of 4 trials per day and error bars represent standard deviation. Statistical analyses are described in the text. Separate groups of sham and brain-injured animals were tested at the two post-injury times.
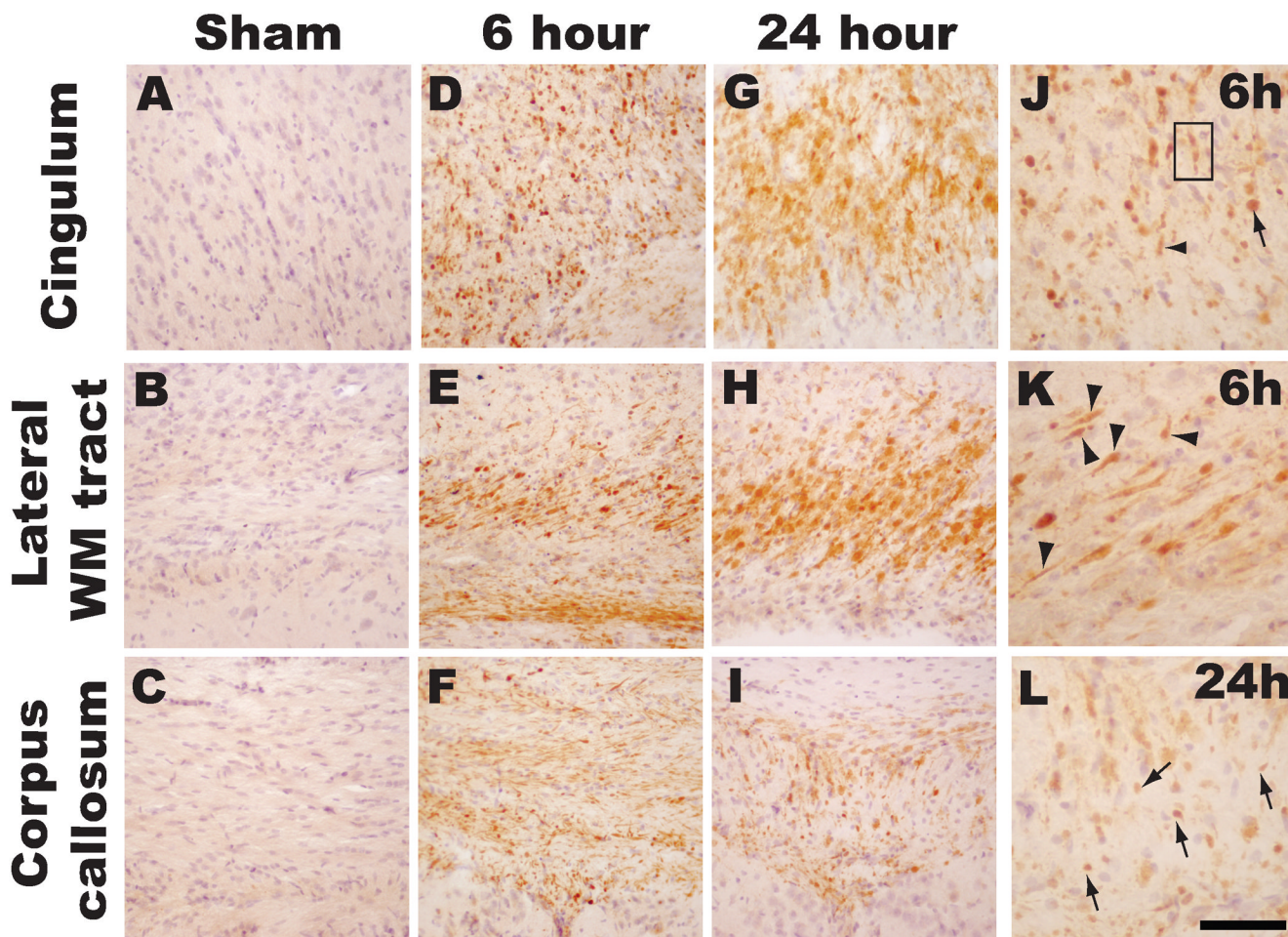
Figure 2. Traumatic axonal injury following midline brain injury in PND17 rats
Sham-injured animals did not have evidence of traumatic axonal injury (A–C). Intra-axonal accumulation of APP, indicative of impaired axonal transport as one phenotype of TAI, was observed at 6 hours (D-F, J, K) and 24 hours (G-I, L) in the cingulum (D, G, J), lateral subcortical white matter tracts (E, H, K), and corpus callosum (F, I, L) in the brain-injured animals. Note APP immunoreactivity in contiguous axons in Figure 2J–L (arrowheads) and in terminal bulbs (arrows). Box in panel J represents multiple foci of APP(+) swellings in a single axon. Scale bar = 200µm for A–I and 100 µm for J-L.
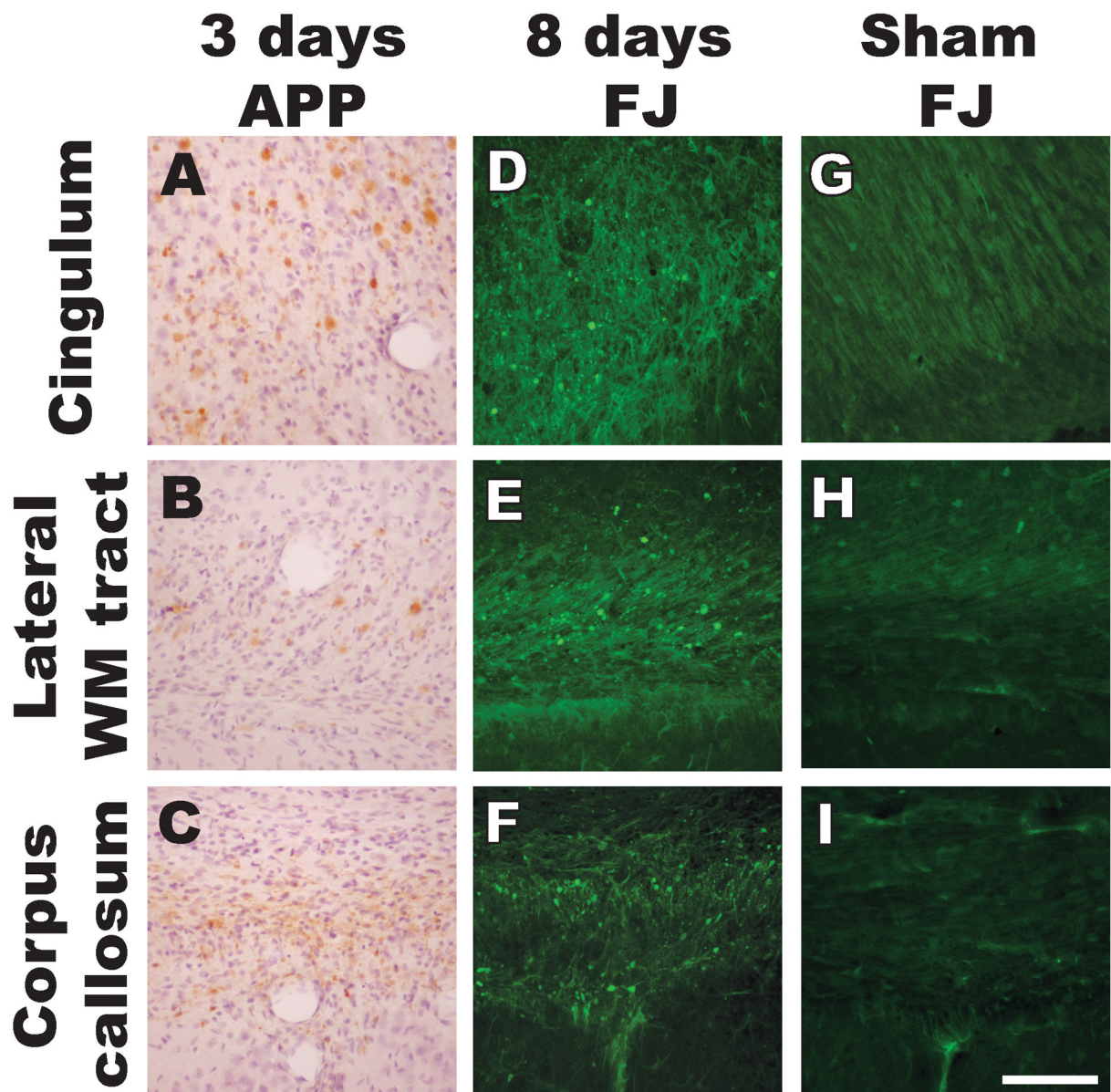
3 days APP   **8 days FJ**   **Sham FJ**

Cingulum   **Lateral WM tract**   **Corpus callosum**

Figure 3. Traumatic axonal injury and axonal degeneration following midline brain injury in PND17 rats

APP accumulation in terminal bulbs was sporadically observed at 3 days post-injury in the cingulum (A), lateral subcortical white matter tracts (B) and corpus callosum (C). At 8 days post-injury, Fluoro-Jade B histochemistry revealed swollen and degenerating axons (indicated by punctate patterns of labeling) in the cingulum (D), lateral white matter tracts (E) and corpus callosum (F). Sham-injured animals did not reveal any Fluoro-Jade B staining in the subcortical white matter tracts (G–I). Scale bar = 100µm for all panels.
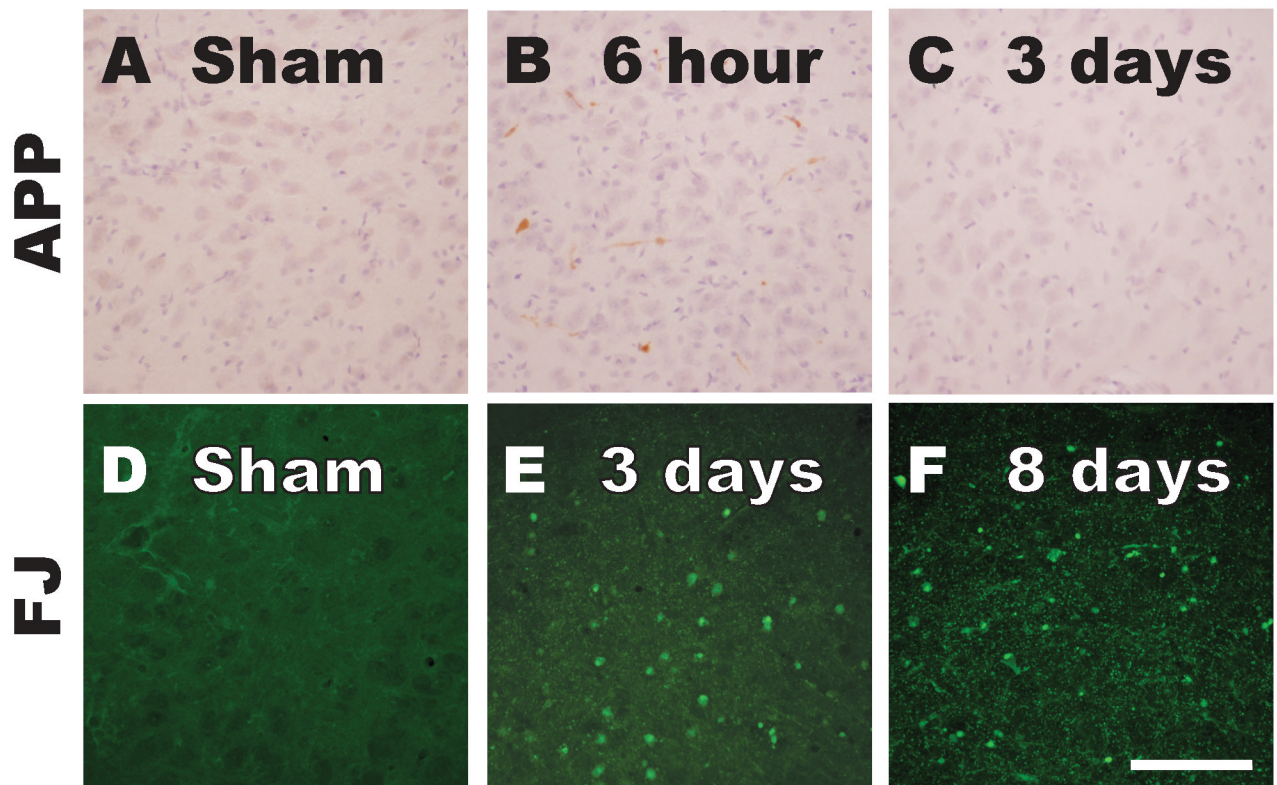
Figure 4. Traumatic axonal injury and degeneration of axons and neuronal cell bodies in the thalamus following midline brain injury in PND17 rats
Accumulation of APP was sporadically observed in thalamic axons at 6 hours (B), but not in sham animals (A) or at 3 days post-injury (C). Compared to sham animals (D), extensive Fluoro-Jade B labeling was present in both axonal profiles and in neuronal cell bodies at 3 (E) and 8 days (F) post-injury. Scale bar = 100µm for all panels.
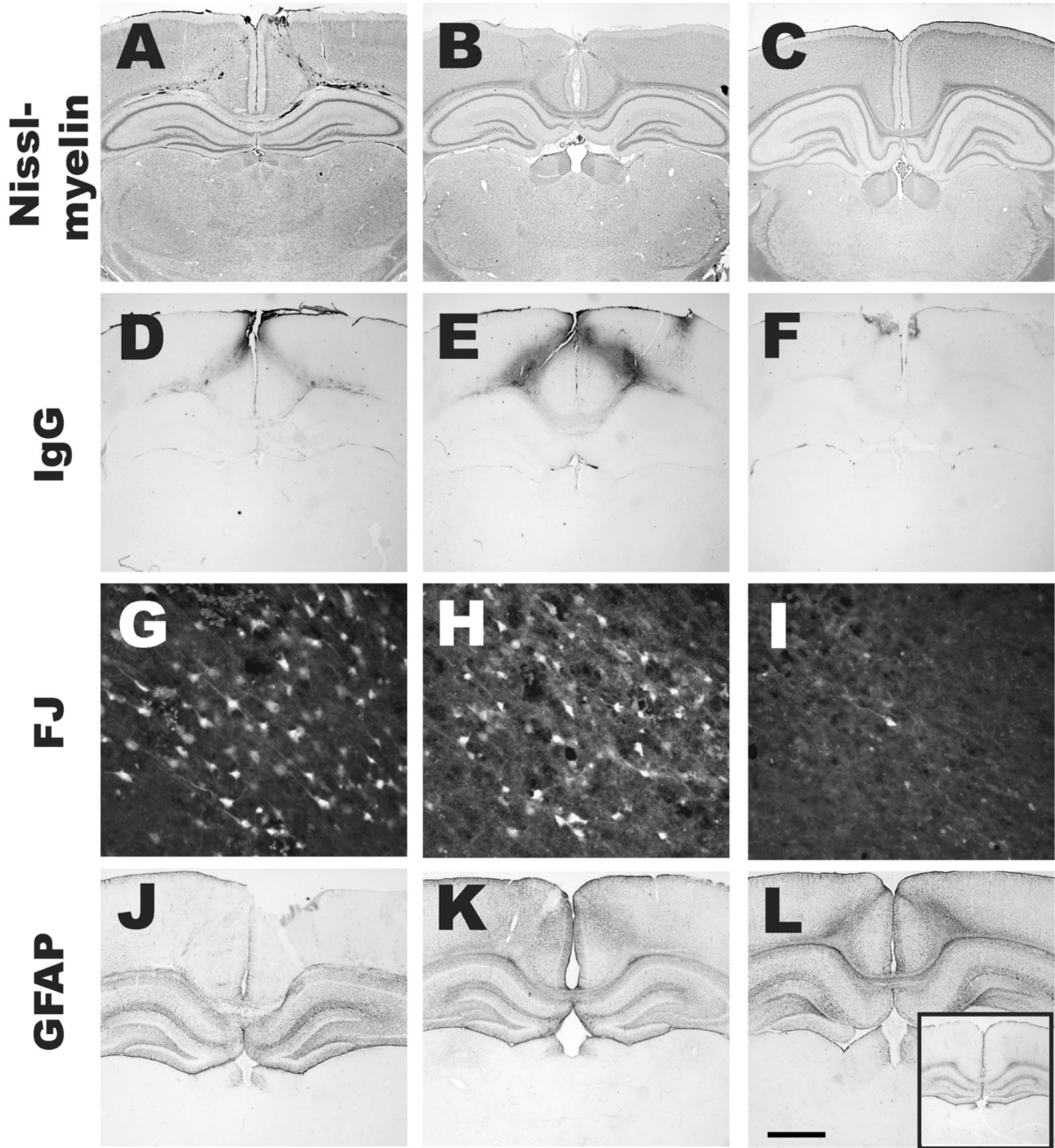
Figure 5. Histopathologic alterations in both hemispheres following midline brain injury in PND17 rats
Nissl-Myelin stained sections (A–C) revealed subpial and intraparenchymal hemorrhage, and, cortical and white matter tissue tears below the site of impact in both hemispheres at 6 hours (A). By 3 days (B), no hemorrhage was observed and by 18 days (C), both hemispheres looked morphologically normal without any evidence of contusion or demyelination of the white matter tracts. IgG immunoreactivity (D–F) within gray and white matter tracts, indicative of blood-brain barrier (BBB) breakdown, was observed at 6 hours directly below the impact site (D), was maximal at 24 hours (E), and was substantially decreased by 3 days post-injury (F). In areas containing hemorrhage and BBB breakdown, Fluoro-Jade B-labeled degenerating

neurons were observed in the injured cortex at 6 (G) and 24 hours (H) and to a lesser extent at 3 days post-injury (I). Reactive astrogliosis was observed in the cortex of both hemispheres at 3 (K) and 8 days (L), but not at 24 hours (J) post-injury, nor in the sham-injured animal (inset in L). Scale bar = 1.6mm for A–F and J–L (including the inset), and 80µm for G–I.
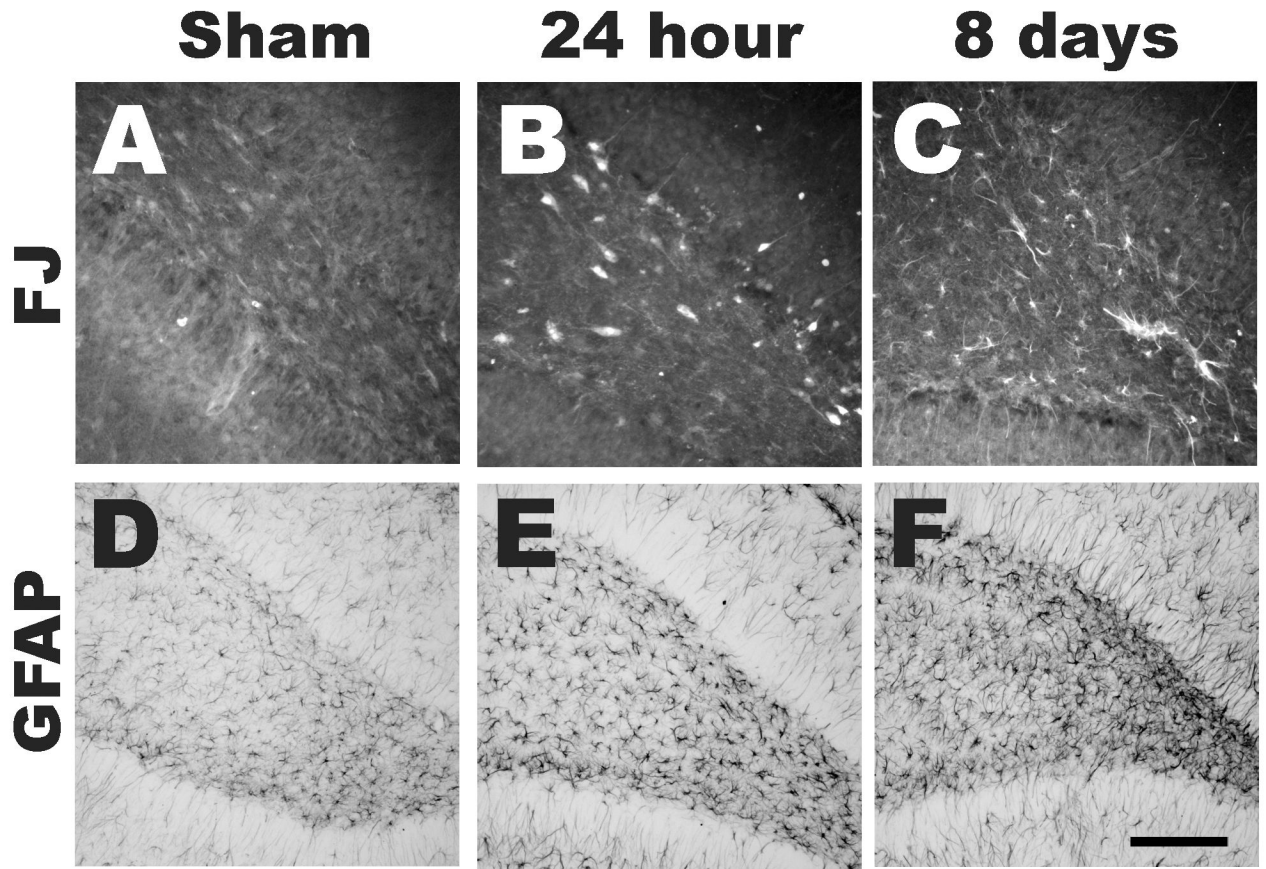
Figure 6. Neurodegeneration in the hippocampus following midline brain injury in PND17 rats
Fluoro-Jade B-labeled neurons were observed in the hilus and the granule cell layer of the hippocampal dentate gyrus at 24 hours post-injury (B). However, in sham animals (A) and at 8 days post-injury (C), Fluoro-Jade B reactivity was observed in cells within the hilus that exhibited non-neuronal morphology. However, the extent of reactive astrogliosis in the hilus of the dentate gyrus was qualitatively similar between sham animals (D) and brain-injured animals at 24 hours (E) and 8 days post-injury (F). Scale bar = 100µm for A–C and 200µm for D–F.
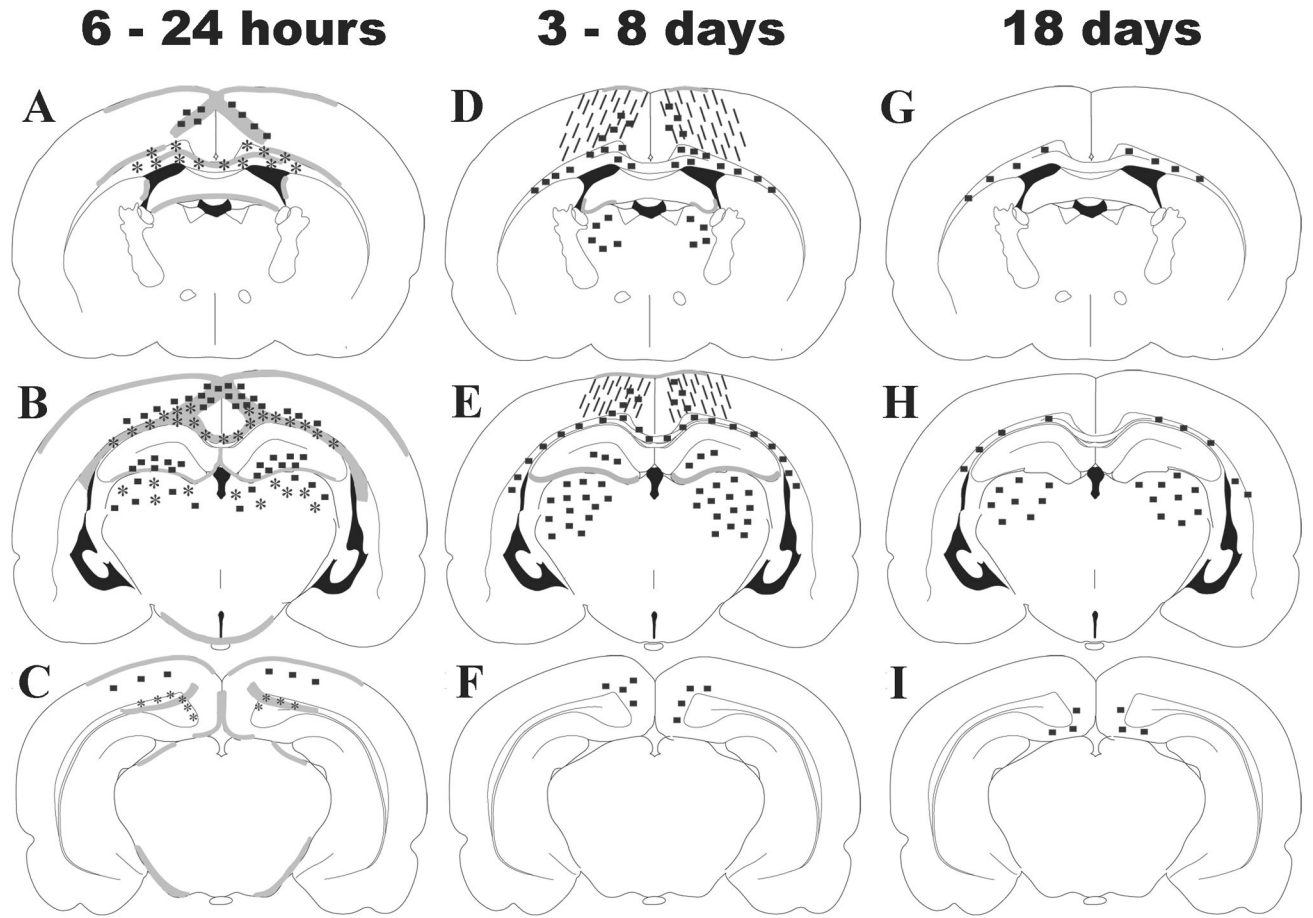
6 - 24 hours

3 - 8 days

18 days

Figure 7. Regional and temporal progression of histopathologic alterations in both hemispheres following midline brain injury in PND17 rats

At 6 to 24 hours (A–C) post-injury, blood-brain barrier breakdown below the site of impact (gray shaded areas), TAI in the subcortical white matter tracts and thalamus (*), and neurodegeneration in the cortex, hippocampal dentate gyrus and thalamus (■) were observed in both hemispheres. By 3 to 8 days (D–F), reactive astrocytosis in the cortex below the impact site (hatch marks) and Fluoro-Jade B-labeled profiles were present within the white matter tracts and the thalamus. By 18 days (G–I) post-injury, a few Fluoro-Jade B(+) profiles persisted within the white matter tracts and the thalamus in both hemispheres.

Table 1

Summary of animals used in the present study.

Survival time (days)	Injury status	
	Sham	**Injured**
0.25	3 (2m, 1f)	4 (2m, 2f)
1	5 (3m, 2f)	4 (3m, 1f)
3	5 (4m, 1f)	4 injured (3m, 1f)
8	10 (4m, 6f)	13 injured (7m, 6f)
18	10 (6m, 4f)	13 injured (6m, 7f)

All animals at the 6 hour (0.25 days), 1 and 3 day time points, and subsets of animals (@ 8 days: N=5 injured - 1m, 4f – and 6 sham – 3m, 3f; @ 18 days: N=4 injured – 1m, 3f – and 4 sham – 2m, 2f) used in the behavioral analyses were used for histological and immunohistochemical analyses.

Table 2

Acute neurologic status following closed head injury in immature rats.

Survival time (days)	N	Apnea (sec)	Skull fractures (%)	Herniation (%)	Severe Hematoma (%)
Shams (all time points)	33	NA	NA	NA	NA
0.25	4	7 ± 2	100	25	75
1	4	5 ± 0	100	0	100
3	4	7 ± 3	100	0	100
8	13	11 ± 8	100	8	92
8 (histology)	5	6 ± 2	100	20	80
18	13	7 ± 2	100	23	77
18 (histology)	4	7 ± 1	100	0	100

Immediately following impact, rat pups were placed on a heating pad and the time of loss of breathing (apnea), pain reflex or righting reflex were evaluated. Once normal breathing was resumed, pups were re-anesthetized with 5% isofluorane in 100% oxygen, and the presence of skull fractures, herniation of the brain and hematoma were recorded. Hematoma was defined based on the presence and location of a discoloration under the skull by visual observation, while herniation was evident from the extrusion of brain tissue through the fracture. Times of apnea are presented as mean ± standard deviation.

Table 3

Cognitive function in sham- and brain-injured rat pups.

Status	Tested on post-injury day	Probe score	Latency to visible platform (s)	Swim Speed (cm/s)
Sham (n=10)	8	127 ± 69	10 ± 8	23 ± 5
Injured (n=13)	8	88 ± 46	24 ± 12	26 ± 11
Sham (n=10)	18	142 ± 62	8 ± 6	22 ± 3
Injured (n=13)	18	98 ± 27[*]	17 ± 18	27 ± 12

Following the 4 days of learning trials (4 trials/day), rats were tested for retention of the location of the platform at 24 hours following the last trial day as described in Methods. Probe scores were calculated from the times spent in the various pre-designated zones as described in Methods. The visible platform trial was conducted immediately after the probe trials.

[*] p<0.05 compared to sham animals. All values are presented as mean ± standard deviation.